Preprints.org

Article

Stat3 Inhibitors TTI-101 and SH5-07 Suppress Bladder Cancer Cell Survival In 3D Tumor Models

Surya Pratap Singh , Gopal Pathuri , Adam S Asch , Chinthalapally V. Rao , Venkateshwar Madka [*]

Article

Stat3 Inhibitors TTI-101 and SH5-07 Suppress Bladder Cancer Cell Survival in 3D Tumor Models

Surya P Singh [1,2], **Gopal Pathuri** [1,2], **Adam Asch** [2], **Chinthalapally V. Rao** [1,2] **and Venkateshwar Madka** [1,2,*]

1   Center for Cancer Prevention and Drug Development, Stephenson Cancer Center, Hem-Onc Section, Department of Medicine, University of Oklahoma HSC, Oklahoma City, OK

2   Stephenson Cancer Center, Hem-Onc Section, Department of Medicine, University of Oklahoma HSC, Oklahoma City, OK

*   Correspondence: vmadka@ouhsc.edu

Abstract: Bladder cancer (BC) is one of the most lethal genitourinary malignancies owing to its propensity for recurrence and poor survival. The biochemical pathway, signal transducer and activator of transcription 3 (STAT3), has gained significance as a molecular pathway that promotes proliferation, invasion, and chemoresistance. In this study, we explored the targeting of STAT3 with TTI-101 and SH5-07 in bladder cancer (BCa) and elucidated the mechanisms in three-dimensional (3D) spheroid and tumoroid models. We optimized the growth of spheroids from human, rat, and mouse BCa cell lines (J82, NBT-II, and MB49, respectively), and tumoroids from BBN (N-butyl-N-(4-hydroxybutyl)-nitrosamine) induced rat bladder tumors. Cell viability was assessed using MTT and trypan blue assays. ATP production, ROS production, and calcium AM (CA)/EtBr staining were used to measure the spheroid and organoid inhibition and mitochondrial function. Western blot analysis was performed to evaluate the pharmacodynamic markers involved in cell proliferation, apoptosis, cancer stem cells (CSCs), and STAT3 signaling in BCa. We found that targeting STAT3 (using TTI-101 and SH5-07) significantly reduced the proliferation of BCa spheroids, and tumoroids, which was accompanied by decreased expression of pSTAT3, Cyclin D1, and PCNA. Our data also demonstrated that treatment with STAT3 inhibitors induced ROS production and cell death in BCa spheroids and organoids. STAT3 inhibition induced cell death was associated with the activation of caspase 3/7 and PARP cleavage. Moreover, TTI-101 and SH5-07 targets cancer stem cells by downregulating the expression of CD44 and CD133 in 3D models. This study provides the first evidence for the prevention of bladder cancer with small-molecule inhibitors TTI101 and SH5-07 via suppression of CSCs and STAT3 signaling.

Keywords: bladder cancer, STAT3 inhibitor, apoptosis, preclinical, 3D models

1. Introduction

Bladder cancer (BCa) is the 10th most common malignancy worldwide [1]. In the United States, 82,290 new cases and 16,710 cancer-related deaths are projected to occur in 2023 [2]. Despite recent advances in its treatment, including chemotherapy, immunotherapy, and surgery, the survival rate of patients with metastatic BCa remains poor. Over the past few years, new strategies have emerged for the management of advanced BCa. For instance, the FDA has approved the immune checkpoint inhibitors PD1/PD-L1 for the treatment of BCa. Unfortunately, many patients do not respond to these immune checkpoint inhibitors [3]. Therefore, platinum-based chemotherapy remains the most effective treatment for patients with advanced metastatic BCa [4]. However, after treatment, many patients experience a significant rate of tumor recurrence. Therefore, there is an urgent need to improve existing BCa management options and develop novel treatment strategies to intercept or delay BCa progression and improve survival rates.

STAT3 (signal transducer and activator of transcription 3) proteins are intracellular transcription factors that regulate several cellular processes including proliferation, apoptosis, EMT, stemness, and immune escape. STAT3 activity is tightly regulated during normal physiology in nonmalignant cells, but it is chronically active in almost 70% of solid tumors [5,6]. STAT3 activation involves

phosphorylation of Tyr705, a critical tyrosine residue that causes STAT3 to undergo homo- or heterodimerization, which facilitates its nuclear localization and DNA binding [7]. Consequently, downstream gene transcription is initiated, which controls essential biological functions.

Studies have reported that bladder malignancies are associated with constitutive STAT3 activation [8]. A growing body of evidence indicates that persistence of CSCs is responsible for tumor development, recurrence, metastasis, chemoresistance, and radio-resistance [9]. Activated STAT3 requires co-expression of Oct3/4 and Nanog, markers of pluripotent stem cells [10]. As a result of these signaling pathways, CSCs markers such as CD44 are upregulated, which increases the niche of CSCs [11,12]. Furthermore, CD133 levels were positively correlated with poor prognosis and tumor growth in patients with BCa [13]. Therefore, STAT3 is considered a promising target for intercepting BCa recurrence and progression. A wide variety of STAT3 activation inhibitors have been reported, including peptides, small molecules, and oligonucleotides [14]. Among these, small molecule inhibitors such as GLG-302 [15], TTI-101 [16], and SH5-07 [17] are designed to abrogate the phosphorylation and dimerization of STAT3. SH5-07 is shown to inhibit the proliferation of breast cancer, human glioma, and prostate cancer cells by decreasing the expression of Bcl-2, Bcl-xL, Mcl-1, cyclin D1, and c-Myc [17]. Similarly, STAT3 inhibitor, TTI-101, has been shown to have potent anticancer effects in preclinical animal models [16]. Unfortunately, due to various limitations, only a few of these agents could progress to an early phase clinical study.

Many preclinical drug development studies used cancer cell lines grown in 2D culture. Studies have shown that cancer cells exhibit altered biological characteristics, including genetic expression, biological activity, and loss of heterogeneity depending on culture conditions [18]. Thus, 2D in vitro models are unable to accurately depict the histopathological characteristics of human diseases limiting the translational relevance of research findings using this system [19]. Owing to these differences in addition to other limitations, only a few of these could progress to an early phase clinical study. Recently, three-dimensional in vitro models have gained popularity for drug development because they closely mimic in vivo environments under heterogeneous and physiological conditions to a certain extent [20]. To the best of our knowledge, this is the first study to examine the anti-cancer mechanisms of STAT3 inhibition by TTI-101 and SH5-07 on BCa spheroids and tumoroids.

2. Materials and Methods

2.1. Cell Culture

Human bladder carcinoma (J82; ATCC Cat # HTB-1), rat bladder carcinoma (NBT-II; ATCC Cat # CRL-1655), and mouse bladder carcinoma (MB49; Accegen Cat # ABC-TC2235S) cell lines were purchased from commercial sources. J82 and NBT-II cells were grown in EMEM; and MB49 cells were grown in DMEM supplemented with 10% FBS and 1% penicillin-streptomycin at 37°C in a 95% humidified atmosphere with 5% CO_2 and maintained by subculturing the cells twice a week. STAT3 inhibitors (GLG 302, TTI-101, and SH5-07) were obtained from the NCI-DCP repository (Figure 1A–C).
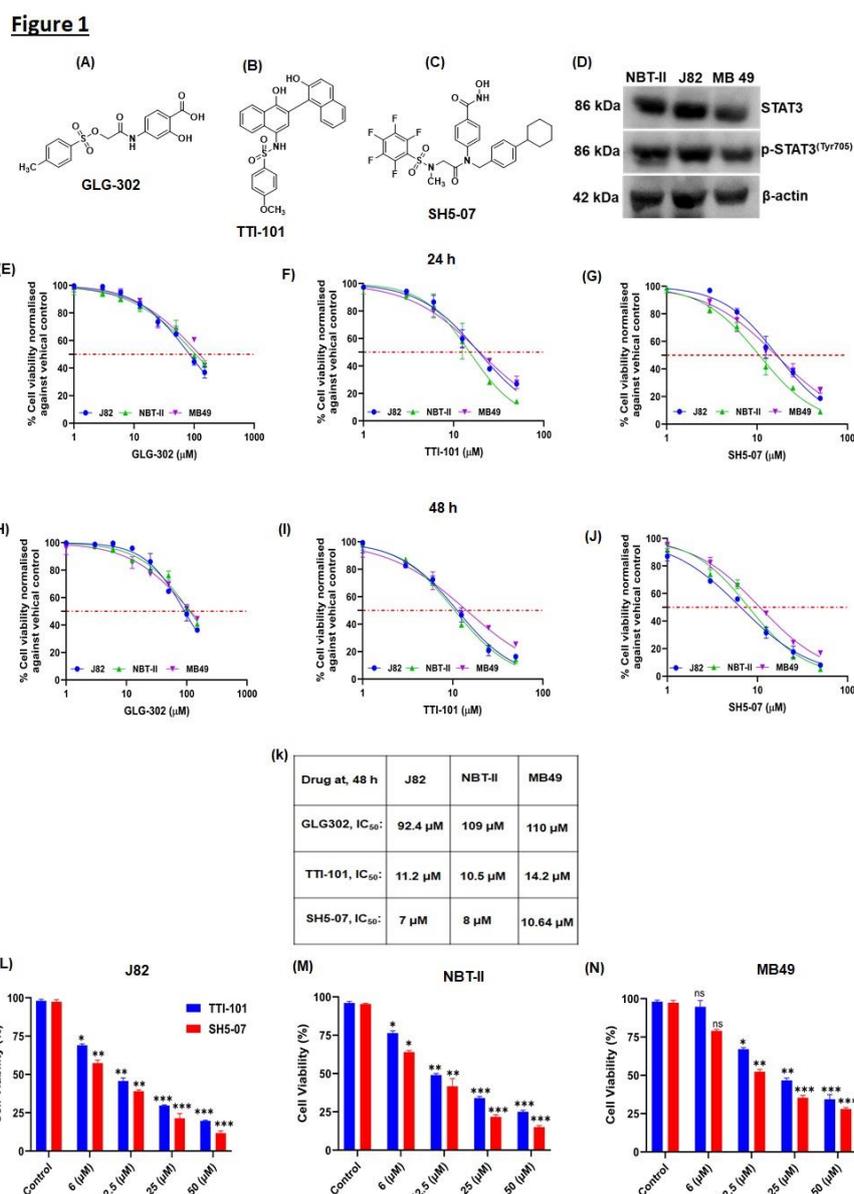
Figure 1. Effect of STAT3 inhibitors on the growth and viability of bladder cancer J82, NBT-II, and MB49 cells. Chemical structure of STAT3 inhibitors (A) GLG-302, (B) TTI-101, and (C) SH5-07. (D) Basal expression levels of STAT3 and pSTAT3 in BCa cell line (NBT-II, J82, and MB49). (E-J) MTT assay was used to determine the viability of BCa cells at 24h and 48 h, as shown in graphs. (K) IC50 values of compounds on NBT-II, J82, and MB49 cells at 48 h of treatment. Cells were cultured with various doses of STAT3 inhibitors (1-50 µM) and processed for the MTT experiment, as detailed in the Materials and Methods. BCa cells were treated with different concentrations of STAT3 inhibitors (0, 6, 12.5, 25, and 50 µM) for 48 h and live cells were counted using the trypan blue dye exclusion method (K-M). The results are representative of three independent experiments. Bars, SEM; *, $P<0.05$; **, $P<0.001$; ***, $P<0.0001$.

2.2. MTT Assay

J82, NBT-II, and MB49 cells were seeded at a density of 8×10^3 cells per well in a 96-well culture plate (Corning Costar, Corning, NY, USA) using standard protocol [21]. After 24 h, cells were treated with STAT3 inhibitors (GLG-302, TTI-101, and SH5-07) at concentrations ranging from 0-50 µM for 24 and 48 h, followed by MTT (Sigma-Aldrich, USA) assays. A standard microplate reader was used to detect the optical density (OD) at 570 nm (Scientific Multiskan MK3, Thermo Fisher Scientific, Waltham, MA, USA).

2.3. Cell Growth and Death Assay

Briefly, 1×10^5 cells were seeded in each 60-mm culture dish and incubated overnight. Cells were treated with GLG-302, TTI-101, and SH5-07 at concentrations 0, 6, 12.5, 25, and 50 µM for 48 h. After the treatment, cells were collected by trypsinization and washed twice with PBS. Then cells were gently mixed with trypan blue dye (Sigma-Aldrich, USA) and counted using TC20 automated cell counter (Bio-Rad).

2.4. Spheroids Culture

J82, NBT-II, and MB49 spheroids were generated using a simple and repeatable procedure that yielded a single spheroid in a single well. BCa cells were grown as a monolayer, trypsinized, and washed. Cells were concentrated and seeded at 1.5×10^3 cells/well in 96-well ultra-low attachment (ULA) plates with 200 µL of complete medium, allowing the cells to assemble into compact 3D aggregates. Every second day, the medium was carefully replaced with fresh medium without disturbing the spheroid growth. A bright-field microscope was used to monitor spheroid growth over a period of 12 days.

2.5. Tumoroids Culture

Carcinogen induced BCa rat model development was approved by IACUC of the University of Oklahoma HSC (Protocol # 23-052). BCa was induced in female F344 rats by oral administration of bladder specific carcinogen, N-Butyl-N-(4-hydroxybutyl) nitrosamine (BBN) following standard protocol [22]. Bladder tumor tissue from the BBN-induced rat BCa model was collected at termination and cut into small pieces (1–2 mm) in PBS with a sterile surgical blade. Tumor pieces were placed in 1 mg/mL collagenase solution in advanced Dulbecco's modified DMEM/F-12 media with ROCK inhibitor (MedChemExpress # Y-27632,). Tissue was incubated at 37°C for 30-minute periods while shaking. Following incubation, the cell suspension was filtered through a 70-micron filter, and the cells were collected by centrifugation at 1800 rpm for 5 min. 1×10^5 cells were mixed with 1 ml of basement membrane extract (BME) and plated in individual wells of a pre-warmed 24-well plate. When the BME solidified, DMEM/F-12 medium supplemented with 100 ng/mL of FGF10 (Peprotech # 100-26), 25 ng/mL of FGF7 (Peprotech # 100-19), A83-01(MedChemExpress # HY-10432) 500 nM, ROCK inhibitor (MedChemExpress # Y-27632,) and B27 (Gibco # 17504044) was added, and the cells were incubated in CO_2 incubators. Bright-field microscopy was used to observe the growth of tumoroids after 24 h of incubation.

2.6. Growth and Viability Assay

To measure the growth kinetics, spheroids were grown for 12 days on ULA plates without treatment. Images of spheroids and organoids were obtained using a microscope. ImageJ software (National Institutes of Health, Bethesda, MD, USA) was used to measure spheroid size. For viability assays, spheroids and organoids were grown in triplicate. Twenty-four hours after seeding, spheroids and organoids were treated with DMSO or STAT3 inhibitor for 144 h. CellTiter-Glo® 3D luminescent assay (Promega, USA) was then used to assess cell viability. Dose-response curves were plotted using GraphPad Prism 8 (GraphPad Software, San Diego, CA, US).

2.7. Calcein AM/EtBr Dual Staining

Spheroids and tumoroids were generated as described above; 24 h after cell seeding, drug treatment was performed for 6 days. At the end of the treatment period, the spheroids were rinsed with 1X PBS, pH 7.4 and then incubated with calcein-AM (Invitrogen™ # C1430) and EtBr (Invitrogen™ # 15585011) solutions for 30 min at final concentrations of 2 mM and 4 mM, respectively. After incubation, the spheroids were washed with 1X PBS twice and images were captured with a fluorescence microscope.

2.8. MitoSOX Staining

MitoSOX staining assay was performed to measure the production of mitochondrial ROS in BCa spheroids and tumoroids. Spheroids and tumoroids were incubated with STAT 3 inhibitors for six days. After incubation, spheroids and tumoroids were stained with 5 μM MitoSOX (Invitrogen™ # M36008) red dye, protected from light for 30 min. Spheroids and tumoroids were washed with PBS to remove any residual dye and images were recorded using fluorescence microscopy.

2.9. MitoTracker and Caspase 3/7 Staining

BCa spheroids and tumoroids were treated with a known concentration of STAT3 inhibitors (TTI-101 and SH5-07) for six days. Later they were incubated with a staining buffer containing MitoTracker (Invitrogen™ # M7512) red and CellEvent Caspase-3/7 (Invitrogen™ # C10423) green. Fluorescence images captured using a fluorescence microscope were processed using ImageJ software.

2.10. Cell Lysis and Immunoblotting

At the completion of the treatment, bladder cancer cells, spheroids, and organoids were lysed with radioimmunoprecipitation assay (RIPA) cell lysis buffer (Thermo Fisher Scientific, USA) containing protease and phosphatase inhibitors. Protein was quantified using the Pierce™ BCA protein assay kit (Thermo Fisher Scientific, USA) and 10-20 μg of protein per lane was resolved on an 8 -10 % SDS-PAGE gel then transferred onto a PVDF membrane. Membranes were incubated with primary and secondary antibodies to determine the expression of various proteins. The following primary antibodies STAT3 (CST-30835, 1:1000), p-STAT3 (CST-9145, 1:1000), Cyclin D1(CST-55506, 1:1000), PCNA (CST-13110, 1:1000), caspase 3 (CST-9662, 1:1000), cleaved PARP (CST-5625, 1:1000), CD44 (CST-37259, 1:1000), and CD133 (AB-A0219, 1:1000) and Rabbit secondary antibody (CST-7074, 1:10000) were used. Enhanced chemiluminescence was detected using a Gbox instrument (Syngene, Bangalore, India). ImageJ software was used to scan the bands, and densitometry was performed.

2.11. Statistical Analysis

All experiments were performed thrice with duplicate samples from each treatment group. Data are presented as Mean+SEM. Significant differences between treatments are analyzed using students' t-test with Welch's correction. The level of significance is presented by * $P < 0.05$, **$P < 0.001$, ***$P < 0.0001$.

3. Results

3.1. p-STAT3 inhibition suppresses the proliferation of BCa cells.

Protein expression analysis indicated that all the BCa cell lines [human (J82), rat (NBT-II), and mouse (MB49) origin] used here have basal expression of STAT3 and pSTAT3^{Y705} enabling us to evaluate STAT3 inhibitors activity (Figure1D). To study the effect of STAT3 inhibition on BCa cell growth and survival, promising STAT3 inhibitors i.e., GLG-302, TTI-101, and SH5-07 were evaluated in vitro by treating BCa cell line with these drugs at 0, 1, 3, 6, 12.5, 25, and 50 μM concentration for 24 and 48 h. Results indicated that TTI-101 and SH5-07 (IC50 ranges 7-14.2 μM) had a strong inhibitory effect on the proliferation of J82, NBT-II, and MB49 cells as compared to GLG-302 that had a moderate effect even at higher concentrations (Figure 1E–J). Further, cell viability analysis using Trypan-blue assay of drug treated BCa cell lines also confirmed a strong anti-cancer effect of STAT3 inhibitors (Figure 1L–N). Based on these findings, TTI-101 and SH5-07 were selected for further investigation on BCa using spheroid and tumoroid models.

3.2. p-STAT3 Inhibitors Suppressed BCa Growth in 3D Spheroid Models

Prior to drug testing, we optimized spheroid growth using J82, NBT-II, and MB49 BCa cell lines. For this, cells were seeded into ULA plates, and the spheroid formation and size were monitored at regular intervals for 12 days under a microscope. All 3 cell lines formed condensed and spherical spheroids (Figure 2A–C). During 14 days of observation, J82 and NBT-II spheroids increased up to 6 days later it remained stable, however, MB49 cells formed less compact spheroids (Figure 2D).

Spheroids generated were treated with STAT3 inhibitors (TTI-101 and SH5-07) and their viability was determined by measuring their diameters and intracellular ATP content (Figure 2E). We observed a significant decrease in the spheroid viability (20%-40%, p<0.0001) (Figure 2F–H) as well as decrease in BCa spheroids size in response to TTI-101 and SH5-07 treatment (Figure 2I–K). MB49 spheroids showed decreased proliferation (Figure 2H) (10–25%, p<0.001), however, the spheroid diameter was less effected due to diffused growth characteristics (Figure 2K). Thus, MB49 spheroids were excluded from further experiments. CA and EtBr staining indicated that TTI-101 and SH5-07 treatment enhanced cell death in BCa spheroids compared to the control (Figure 2L–M). These results demonstrate that TTI-101 and SH5-07 suppressed the growth of BCa spheroids.
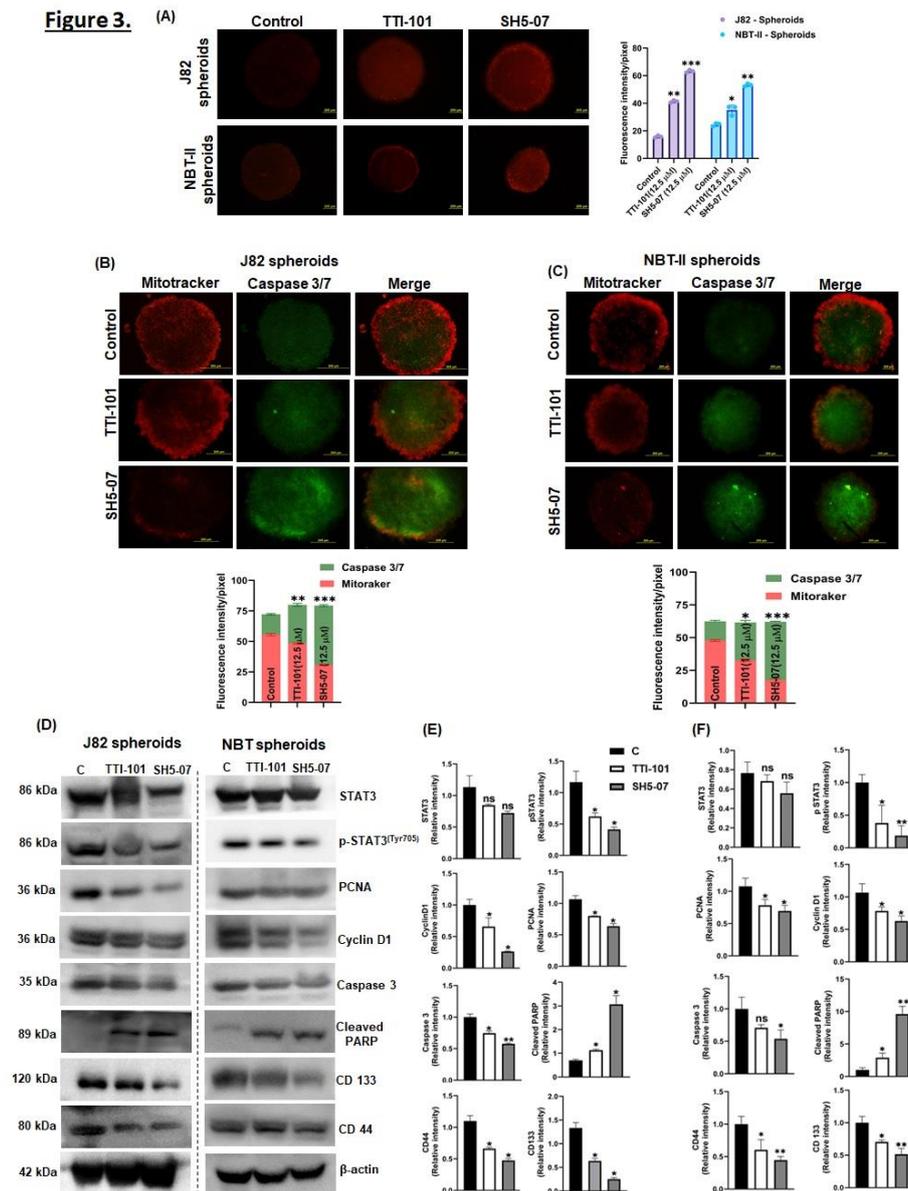
Figure 2
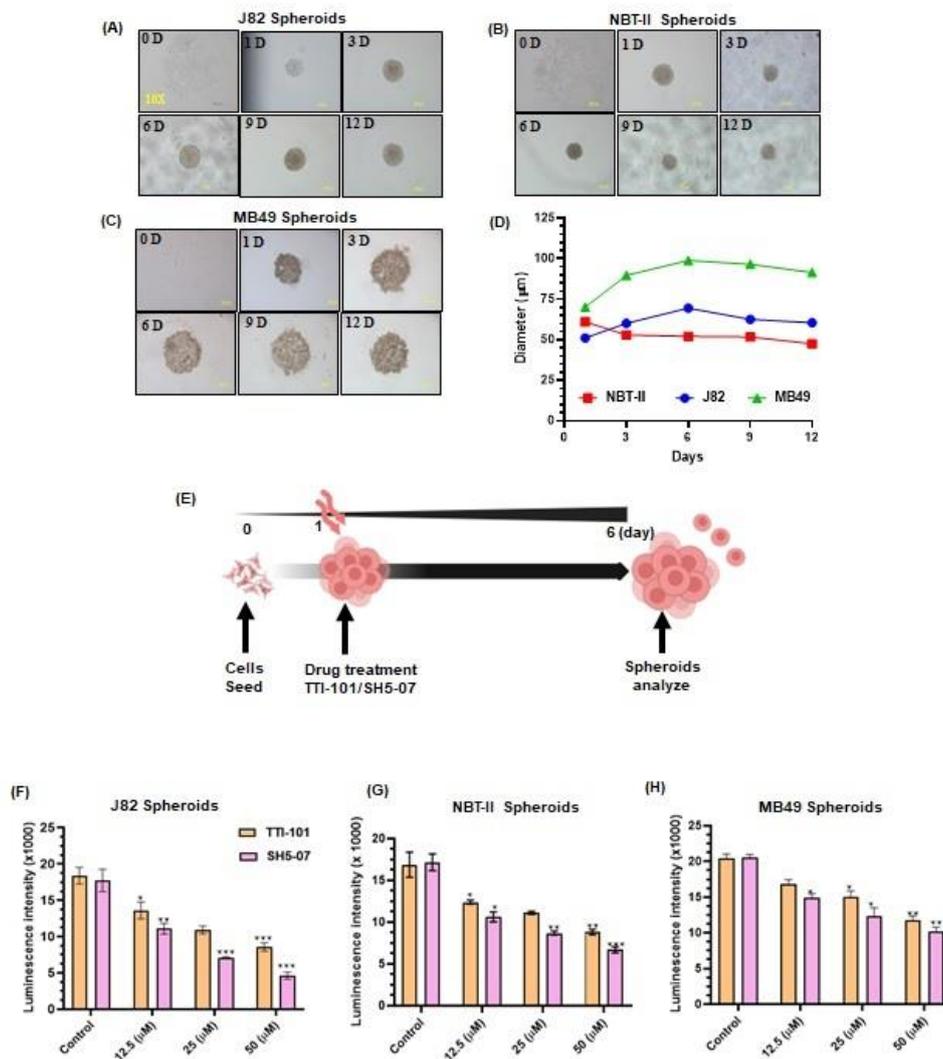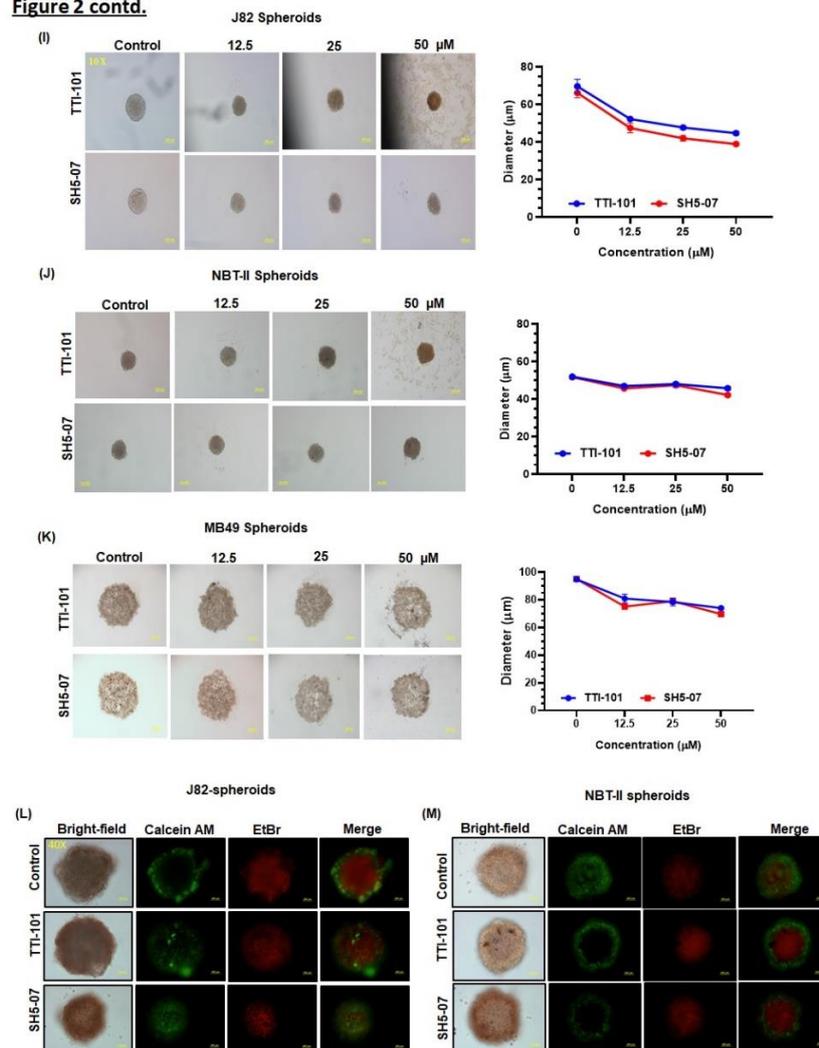
Figure 2. Effect of STAT3 inhibitors on proliferation of BCa spheroids. Representative images of spheroids generated using J82 (A), NBT-II (B), and MB49 (C) BCa cell lines. All images were captured at a 10X magnification. Growth curves of spheroid sizes (D). Schematic diagram illustrating treatment of spheroids with STAT3 inhibitors (E). Intracellular ATP content in (I-K) spheroids measured by luminescence on day six (F-H). Treatment with STAT3 inhibitors decreased the BCa spheroids size (I-K). Spheroids were stained with Calcein AM for live cells (green) and EtBr for dead cells (red). Representative images of control vs. treated BCa spheroids (L-M). All experiments were performed in triplicate (n=3). Values are expressed as the mean ± SEM. Significance is indicated by *P < 0.05, **P < 0.001, and ***P < 0.0001.

3.3. p-STAT3 Inhibition Enhanced Apoptosis via Mitochondrial ROS Induction, and Inhibited Stemness in BCa Spheroids

Activation of ROS is known to interfere with apoptosis induction; therefore, we examined whether mitochondrial ROS played any role in TTI-101 and SH5-07-induced apoptosis in BCa spheroids. The ROS generation within BCa spheroids was quantified by staining BCa spheroids with MitoSOX Red dye. It was observed that SH5-07 induced significant mitochondrial ROS production in both BCa spheroids as compared to TTI-101 (Figure 3A). Further, MitoTracker and caspase-3/7 staining was used to determine apoptosis induction in BCa spheroids in response to TTI-101 and SH5-07 treatment. In live cells, the mitochondrial staining dye MitoTracker diffuses passively across the plasma membrane and accumulates in active mitochondria, whereas caspase-3/7 stains apoptotic cells. The results showed that treatment with TTI-101 and SH5-07 significantly decreased MitoTracker fluorescence intensity while increasing caspase-3/7 intensity in both BCa spheroids (Figure 3B–C)

suggesting that STAT3 inhibitors induced apoptosis in BCa spheroids. Further, we found that STAT3 inhibitors (TTI-101 and SH5-07) significantly reduced the expression of pSTAT3^{Y705}, and cell proliferation-related proteins PCNA and cyclin D1. In addition, J82 spheroids showed more sensitive than NBT-II spheroids to both inhibitors (TTI-101 and SH5-07). Drug treatment also enhanced the expression of apoptosis markers cleaved PARP in both BCa spheroids. The stem cell marker proteins CD44, and CD133 were also downregulated by TTI-101 and SH5-07 treatments (Figure 3D). Collectively, these findings demonstrate that the STAT3 inhibitor SH5-07 more significantly compared TTI-101 to decreased the growth of BCa via ROS-induced apoptosis and suppression of stemness.
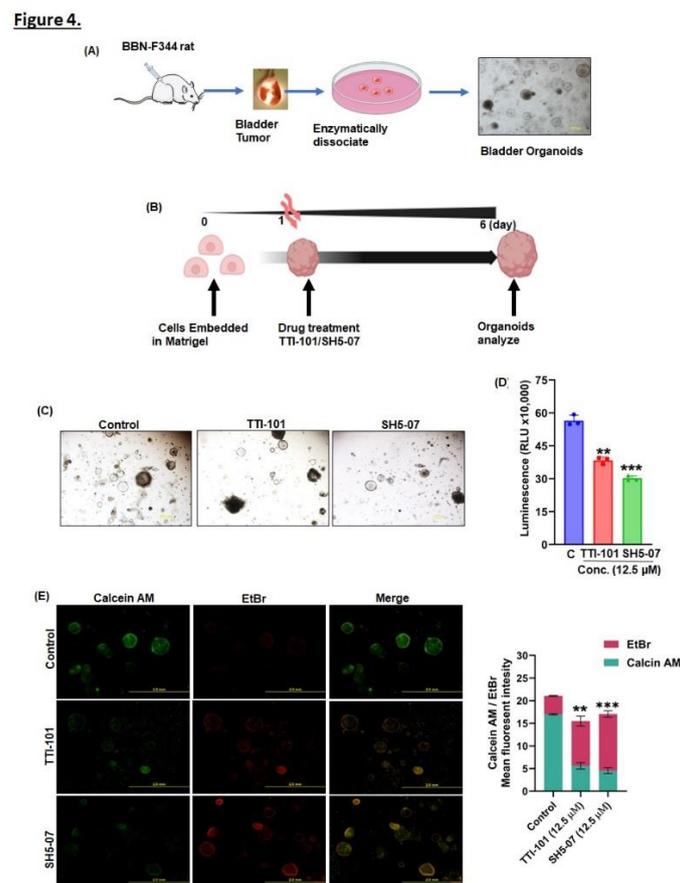

Figure 3. Effect of STAT3 inhibitors on apoptosis induction in BCa spheroids. BCa spheroids were treated with STAT3 inhibitors and then stained with MitoSOX and visualized under a fluorescent microscope (A). Spheroids stained with MitoTracker (red) and CellEvent Caspase-3/7 (green). Images were acquired using 50X objectives (B, C). Western blotting was performed in BCa spheroids treated with 12.5 µM TTI-101 or SH5-07 for 6 days to determine the expression of STAT3, pSTAT3, Cyclind1, PCNA, Caspase 3, cleaved PARP, CD133, CD44. β-actin is used as loading controls (D). The intensity of the indicated protein expression in J82 spheroids and NBT-II spheroids were quantified using the

ImageJ software (E, F). Data represent the average of three independent experiments and are reported as the mean ± SEM (* P < 0.05, **P < 0.001, ***P < 0.0001).

3.4. p-STAT3 Inhibitors Suppressed Rat BCa Tumoroid Growth and Survival

Rat BCa tumoroids were established from freshly collected tumor tissues as described in the methods section (Figure 4A). Next, we assessed the growth of tumoroids by measuring their viability in response to TTI-101 and SH5-07. Our data indicated that TTI-101 treatment reduced 28% (P<0.05) and SH5-07 treatment reduced 31% (P<0.05) the viability tumoroids (Figure 4B–D). Further, we determine the mode of cell death and morphological changes caused by TTI-101 and SH5-07 by staining the tumoroids with dead-live Calein AM/EtBr. Results showed that TTI-101 and SH5-07 induced cell death in treated tumoroids compared to control (Figure 4E).

Figure 4. Effect of STAT3 inhibitors on BBN-induced rat tumor derived BCa tumoroids. Schematic of organoid culture procedure from Rat bladder tumors (A). Overview of the timeframe experiment (B). STAT3 inhibitors (TTI-101 and SH5-07) decreased organoid growth (C). Tumor cell proliferation was measured using the CellTiter-Glo assay after six days of drug treatment (D). Assessment of STAT 3 inhibitors on bladder organoids using ethidium homodimer (dead) and calcein AM (live) staining (E). Values are (n=3) Mean ± SEM (* P < 0.05, **P < 0.001, ***P < 0.0001).

Both agents induced ROS generation, however, SH5-07 appear to be more efficient than TTI-101 (Figure 5A). We also found that TTI-101 and SH5-07 treatment increased caspase3/7 activity and decreased MitoTracker intensity compared to untreated organoids (Figure 5B).
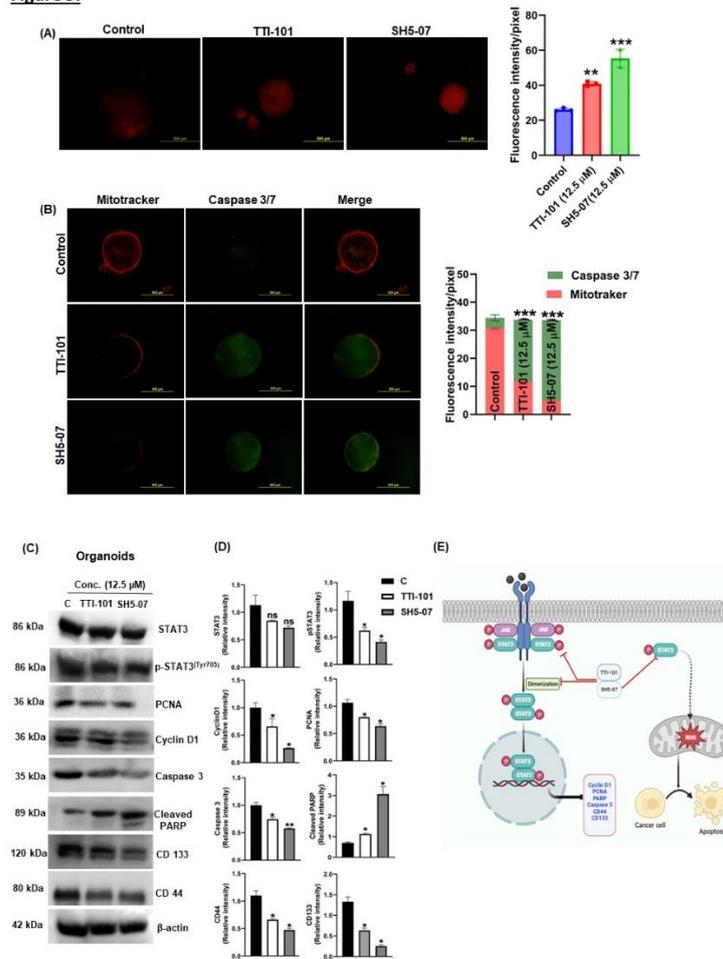
Figure 5. Effect of STAT 3 inhibitors on apoptosis induction in BCa organoids. Fluorescence staining of mitochondrial superoxide production after treatment with TTI-101 and SH5-07 at concentration 12.5 μM for six days (A). After TTI-101 and SH5-07 treatment, organoids were stained with MitoTracker (red) and CellEvent Caspase-3/7 (green) to detect cell death within organoids (B). BCa organoids were treated with the STAT3 inhibitor at the indicated doses for 6 days. STAT3, pSTAT3, Cyclind1, PCNA, caspase 3, cleaved PARP, CD133 and CD44 protein expression levels were detected by immunoblotting (C). Densitometric analysis was performed to quantify the protein expression in the BCa organoids(D). Values are (n=3) means ± SE (* P < 0.05, **P < 0.001, ***P < 0.0001). Graphical summary of the molecular effects of the STAT3 inhibitors on BCa cells (E).

Additionally, we verified the effect of TTI-101 and SH5-07 treatment on the expression of proteins involved in proliferation, apoptosis, stem cells, and STAT3 signaling in BCa tumoroids. Results of western blotting showed a decrease in the expression of pSTAT3Y705, the proliferation marker PCNA, and Cyclin D1, which correlated to the reduced BCa tumoroid size (Figure 5C). The apoptosis marker proteins cleaved PARP were significantly increased in BCa tumoroids following treatment with TTI-101 and SH5-07, while the stem cell markers CD44, and CD133 were significantly decreased (Figure 5C). These results imply that inhibition of STAT3 signaling, induction of apoptosis, and decreased stem cell markers could be one of the anticancer mechanisms of TTI-101 and SH5-07 (Figure 5E).

4. Discussion

Recently, significant attention has been paid to developing more predictable cellular models for in vitro screening of anticancer agents. 3D culture models mimic a microenvironment like that found within in vivo tumors, by maintaining the phenotypes and functions of native cells. Mostly, 3D BCa spheroids and organoid models are typically produced from commercial cell lines and bladder tumor

tissues using an ultra-low-attachment plate and Matrigel, respectively [23,24]. Here, we established a spheroid and tumoroid culture method for BCa cells and a BBN-rat bladder cancer model to investigate the molecular mechanisms of small-molecule p-STAT3 inhibitors. The culture approach is based on earlier established spheroids and organoids model of BCa [24,25].

STAT3 is a transcription factor that plays a prominent role in tumorigenesis, making it a valuable target for cancer interception. According to various studies, STAT3 expression levels correlate with invasiveness and poor prognosis in bladder cancer [26,27]. The development of effective inhibitors that target STAT3 signaling has received substantial attention. This study aimed to examine the anti-BCa effects of three promising small-molecule STAT3 inhibitors i.e., GLG 302, TTI-101, and SH5-07 using various preclinical models. Despite the common target, these agents differ slightly in their molecular mechanism of action. GLG-302 inhibits STAT3 DNA-binding activity in vitro and decreases the proliferation of cells with constitutively active STAT3 [15]. TTI-101 is a competitive inhibitor of STAT3 and inhibits STAT3 recruitment and activation by targeting the receptor's pY705-peptide binding site in the SH2 domain [16]. Recently, SMARCB1 (switch/sucrose nonfermentable-related matrix-associated actin-dependent regulator of chromatin subfamily B member 1), which encodes INI-1 (integrase interactor 1) loss was found to drive bladder tumor progression via activation of IL6/STAT3 axis. In this context, pSTAT3 inhibition using TTI-101 was found to suppress the formation of in vivo tumor growth in SMARCB1 KO orthotopic cell line-derived xenografts and a xenograft-derived model from a SMARCB1-deficient patient [28].

SH5-07 is a hydroxamic acid analog that selectively inhibits STAT3 DNA-binding activity [29]. To determine the plausibility of these drugs in BCa cells, we examined the expression of STAT3 in BCa cells and found that all the cell line models expressed STAT3 and p-STAT3, thus, allowing us to assess the anti-tumor effects of STAT3 inhibitors. Similar to earlier reports, we observed a strong anti-cancer effect of STAT3 inhibition [30]. Interestingly, the level of inhibition of the 3 agents correlated with target expression levels with stronger inhibition of the J82 and NBT-II cell lines with higher levels of STAT3 compared to MB49. Comparing the size of spheroids and organoids exposed to a test compound is regarded as one of the best ways to assess the impact of a drug on tumor cells in a 3D environment [31,32]. Here, we observed a decrease in BCa spheroids and tumoroids size in response to STAT3 inhibitors treatment implying that disrupting STAT3 inhibits cell proliferation in 3D cultures. This finding also supported the concept that reduced spheroids and tumoroid size correlated with decreased spheroids and organoids proliferation [33]. Adenosine triphosphate (ATP) is an important biochemical element in the tumor microenvironment (TME), and its concentration influences tumor growth [34]. It is reported that the increased production of ATP accelerates the proliferation of cancer cells, which is strongly controlled by STAT3 activation [35].

In cells, mitochondria are believed to be the major source of ROS production during oxidative stress, and mitochondrial dysfunction is considered the earliest signal of cell death [36]. It is reported that STAT3 activation is inhibited by ROS production [37]. Interestingly, after treatment with TTI-101 and SH5-07, there was a significant increase in ROS production in BCa cells, indicating that it may also be involved in anticancer effects. Activated STAT3 signaling is known to regulate essential cancer cell mechanisms such as proliferation, survival, and metastasis pathways by modulating genes involved in cell proliferation (PCNA), the cell cycle (Cyclin D1), and apoptosis (PARP and Caspase 3) [38]. Numerous studies have shown that STAT3 activation requires phosphorylation of tyrosine 705 for homodimerization, nuclear translocation, and DNA-binding activity [39]. Here, we observed that TTI-101 and SH5-07 inhibit STAT3 phosphorylation, resulting in the suppression of STAT3-regulated gene products, including PCNA and Cyclin D1. The reduced expression of these two genes after treatment with TTI-101 and SH5-07 could provide an explanation for the anticancer effect of TTI-101 and SH5-07 by blocking STAT3 signaling. Apoptotic cell death is triggered by caspases, which cleaves several proteins crucial for cellular survival and function [40]. PARP-1 is one of several known caspase cellular substrates. The cleavage of PARP-1 by caspases, especially caspase-3 and caspase-7 is thought to be a sign of apoptosis [41]. Our data showed that active caspase-3/7 and PARP cleavage remarkably increased after TTI-101 and SH5-07 treatment in BCa cell lines, spheroids, and tumoroids.

Several studies have reported that STAT3 signaling plays a key role in regulating cancer stem cells (CSCs), unique subpopulations of cells within tumors implicated in chemotherapy resistance [7]. Therefore, we examined the protein levels of the key stem cell markers CD44 and CD133 in BCa [42]. Upon TTI-101 and SH5-07 treatment, the expression of CD44 and CD133 was significantly reduced, whereas these markers were highly expressed in control spheroids and tumoroids. Overall, these results suggest that TTI-101 and SH5-07 may serve as novel therapeutic compounds that suppress CSCs proliferation.

5. Conclusions

The present study showed that pharmacological targeting of p-STAT3 inhibited cell growth in multiple cell culture models of bladder cancer. Our results demonstrated that TTI-101 and SH5-07 have anticancer efficacy against bladder cancer, mediated by p-STAT3 inhibition, apoptosis induction, and stem cell depletion. Based on these encouraging in vitro findings, further in vivo investigations are needed to determine whether this agent could be clinically used for intercepting bladder cancer recurrence and progression.

References

1.   Jubber, I.; Ong, S.; Bukavina, L.; Black, P. C.; Compérat, E.; Kamat, A. M.; Kiemeney, L.; Lawrentschuk, N.; Lerner, S. P.; Meeks, J. J.; Moch, H.; Necchi, A.; Panebianco, V.; Sridhar, S. S.; Znaor, A.; Catto, J. W. F.; Cumberbatch, M. G. Epidemiology of bladder cancer in 2023: A systematic review of risk factors. Eur. Urol. 2023, 84,176-190.

2.   Siegel, R. L.; Miller, K. D.; Wagle, N. S.; Jemal, A. Cancer Statistics, 2023. Ca. Cancer J. Clin. 2023,73,17–48.

3.   Robertson, A. G.; Meghani, K.; Cooley, L. F.; McLaughlin, K. A.; Fall, L. A.; Yu, Y.; Castro, M. A. A.; Groeneveld, C. S.; de Reyniès, A.; Nazarov, V. I.; Tsvetkov, V. O.; Choy, B.; Raggi, D.; Marandino, L.; Montorsi, F.; Powles, T.; Necchi, A.; Meeks, J. J. Expression-Based Subtypes Define Pathologic Response to Neoadjuvant Immune-Checkpoint Inhibitors in Muscle-Invasive Bladder Cancer. Nat. Commun. 2023, 14, 2126.

4.   Gómez De Liaño, A.; Duran, I. The Continuing Role of Chemotherapy in the Management of Advanced Urothelial Cancer. Ther. Adv. Urol. 2018, 10, 455–480.

5.   Turkson, J.; Jove, R. STAT Proteins: Novel Molecular Targets for Cancer Drug Discovery. Oncogene. 2000, 19, 6613–6626.

6.   Levy, D. E.; Inghirami, G. STAT3: A Multifaceted Oncogene Proc. Nat. Acad. Sci. 2006, 103, 10151–10152.

7.   Philip Wing-Lok Ho; Lay, E.; Jian, W.; Parra, D. C.; Keith. Stat3 Activation in Urothelial Stem Cells Leads to Direct Progression to Invasive Bladder Cancer. Cancer Res. 2012, 72, 3135–3142.

8.   Mirzaei, S.; Gholami, M. H.; Mahabady, M. K.; Nabavi, N.; Zabolian, A.; Banihashemi, S. M.; Haddadi, A.; Entezari, M.; Hushmandi, K.; Makvandi, P.; Samarghandian, S.; Zarrabi, A.; Ashrafizadeh, M.; Khan, H. Pre-Clinical Investigation of STAT3 Pathway in Bladder Cancer: Paving the Way for Clinical Translation. Biomed. Pharmacother. 2021, 133, 111077.

9.   Cancer Cells Stemness: A Doorstep to Targeted Therapy. Biochim. Biophys. Acta. Mol. Basis. Dis. 2020, 1866, 165424.

10. Gibbs, C. P.; Kukekov, V. G.; Reith, J. D.; Tchigrinova, O.; Suslov, O. N.; Scott, E. W.; Ghivizzani, S. C.; Ignatova, T. N.; Steindler, D. A. Stem-like Cells in Bone Sarcomas: Implications for Tumorigenesis. Neoplasia. 2005, 7, 967–976.

11. Marotta, L. L. C.; Almendro, V.; Marusyk, A.; Shipitsin, M.; Schemme, J.; Walker, S. R.; Bloushtain-Qimron, N.; Kim, J. J.; Choudhury, S. A.; Maruyama, R.; Wu, Z.; Gönen, M.; Mulvey, L. A.; Bessarabova, M. O.; Huh, S. J.; Silver, S. J.; Kim, S. Y.; Park, S. Y.; Lee, H. E.; Anderson, K. S. The JAK2/STAT3 Signaling Pathway Is

Required for Growth of CD44+CD24– Stem Cell–like Breast Cancer Cells in Human Tumors. J. Clin. Invest. 2011, 121, 2723–2735.

12. Wu, C.-T.; Lin, W.-Y.; Chen, W.-C.; Chen, M.-F. Predictive Value of CD44 in Muscle-Invasive Bladder Cancer and Its Relationship with IL-6 Signaling. Ann. Surg. Oncol. 2018, 25, 3518–3526.

13. Wasfy, R. ES; El-Guindy, D. M. CD133 and CD44 as Cancer Stem Cell Markers in Bladder Carcinoma. Egypt. J. Pathol. 2017, 37, 204–208.

14. Singh, S. P.; Asch, A. S.; Rao, C. V.; Venkateshwar Madka. Bladder Cancer Prevention: Potential Molecular Targets and Their Clinically Relevant Agents. Curr. Pharmacol. Rep. 2023, 9, 275–283.

15. Shoemaker, R.; Fox, J.; Juliana, M.; Moeinpour, F.; Grubbs, C. Evaluation of the STAT3 Inhibitor GLG-302 for the Prevention of Estrogen Receptor-Positive and -Negative Mammary Cancers. Oncol. Rep. 2019, 42, 1205-1213.

16. Kasembeli, M. M.; Singhmar, P.; Ma, J.; Edralin, J.; Tang, Y.; Adams, C.; Heijnen, C. J.; Kavelaars, A.; Tweardy, D. J. TTI-101: A Competitive Inhibitor of STAT3 That Spares Oxidative Phosphorylation and Reverses Mechanical Allodynia in Mouse Models of Neuropathic Pain. Biochem. Pharmacol. 2021, 192, 114688.

17. Yue, P.; Lopez-Tapia, F.; Paladino, D.; Li, Y.; Chen, C.-H.; Namanja, A. T.; Hilliard, T.; Chen, Y.; Tius, M. A.; Turkson, J. Hydroxamic Acid and Benzoic Acid-Based STAT3 Inhibitors Suppress Human Glioma and Breast Cancer Phenotypes in Vitro and in Vivo. Cancer Res. 2016, 76, 652–663.

18. Kapałczyńska, M.; Kolenda, T.; Przybyła, W.; Zajączkowska, M.; Teresiak, A.; Filas, V.; Ibbs, M.; Bliźniak, R.; Łuczewski, Ł.; Lamperska, K. 2D and 3D Cell Cultures – a Comparison of Different Types of Cancer Cell Cultures. Arch. Med. Sci. 2018,14,910-919.

19. Wang, H.; Brown, P. C.; Chow, E. C. Y.; Ewart, L.; Ferguson, S. S.; Fitzpatrick, S.; Freedman, B. S.; Guo, G. L.; Hedrich, W.; Heyward, S.; Hickman, J.; Isoherranen, N.; Li, A. P.; Liu, Q.; Mumenthaler, S. M.; Polli, J.; Proctor, W. R.; Ribeiro, A.; Wang, J.; Wange, R. L. 3D Cell Culture Models: Drug Pharmacokinetics, Safety Assessment, and Regulatory Consideration. Clin Transl. Sci. 202,14,1659-1680.

20. Fang, Y.; Eglen, R. M. Three-Dimensional Cell Cultures in Drug Discovery and Development. SLAS Discov. 2017, 22, 456–472.

21. Thepmalee, C.; Sawasdee, N.; Jenkham, P.; Thephinlap, C.; Khoothiam, K.; Suwannasom, N.; Chokchaisiri, R.; Panya, A.; Yenchitsomanus, P.-T. Anti-Cancer Effect of a Phytochemical Compound - 7R-Acetylmelodorinol - against Triple-Negative Breast Cancer Cells. Biomed Pharmacother. 2023, 1, 166, 115286.

22. Mohammed, A.; Mark Steven Miller; Lubet, R. A.; Suen, C. S.; Sei, S.; Shoemaker, R. H.; Juliana, M. M.; Moeinpour, F. L.; Grubbs, C. J. Combination of Erlotinib and Naproxen Employing Pulsatile or Intermittent Dosing Profoundly Inhibits Urinary Bladder Cancers. Cancer Prev. Res. 2020, 13, 273–282.

23. Wang, Y.; Day, M. L.; Simeone, D. M.; Palmbos, P. L. 3-D Cell Culture System for Studying Invasion and Evaluating Therapeutics in Bladder Cancer. J. Vis. Exp. 2018,139, 58345.

24. Yoshida, T.; Kates, M.; Sopko, N. A.; Liu, X.; Singh, A. K.; Bishai, W. R.; Joice, G.; McConkey, D. J.; Bivalacqua, T. J. Ex Vivo Culture of Tumor Cells from N-Methyl-N-Nitrosourea-Induced Bladder Cancer in Rats: Development of Organoids and an Immortalized Cell Line. Urol. Oncol. 2018, 36, 23–160.

25. Tatokoro, M.; Koga, F.; Yoshida, S.; Kawakami, S.; Fujii, Y.; Neckers, L.; Kihara, K. Potential Role of Hsp90 Inhibitors in Overcoming Cisplatin Resistance of Bladder Cancer-Initiating Cells. Int. J. Cancer. 2011,131, 987–996.

26. Gatta; Melocchi; Bugatti; Missale; Lonardi; Zanetti; Cristinelli; Belotti; Simeone; Ronca; Grillo; Licini; Bresciani; Tardanico; Chan; Giurisato; Calza; Vermi. Hyper-Activation of STAT3 Sustains Progression of Non-Papillary Basal-Type Bladder Cancer via FOSL1 Regulome. Cancers. 2019, 11, 1219.

27. Keith; Espinosa, I.; Chao, M. P.; Wong, D.; Ailles, L.; Diehn, M.; Gill, H.; Presti, J. C.; Chang, H. Y.; Matt; Shortliffe, L. D.; Weissman, I. L. Identification, Molecular Characterization, Clinical Prognosis, and Therapeutic Targeting of Human Bladder Tumor-Initiating Cells. Proc. Natl. Acad. Sci. U S A. 2009, 106, 14016–14021.

28. Amara, C. S.; Kami Reddy, K. R.; Yuntao, Y.; Chan, Y. S.; Piyarathna, D. W. B.; Dobrolecki, L. E.; Shih, D. J. H.; Shi, Z.; Xu, J.; Huang, S.; Ellis, M. J.; Apolo, A. B.; Ballester, L. Y.; Gao, J.; Hansel, D. E.; Lotan, Y.; Hodges, H. C.; Lerner, S. P.; Creighton, C. J.; Sreekumar, A.; Zheng W.J.; Msaouel, P.; Kavuri, S.M.; Putluri, N. The IL6/JAK/STAT3 Signaling Axis Is a Therapeutic Vulnerability in SMARCB1-Deficient Bladder Cancer. Nat. Commun. 2024, 15, 1373.

29. Yue, P.; Lopez-Tapia, F.; Paladino, D.; Li, Y.; Chen, C.-H.; Namanja, A. T.; Hilliard, T.; Chen, Y.; Tius, M. A.; Turkson, J. Hydroxamic Acid and Benzoic Acid-Based STAT3 Inhibitors Suppress Human Glioma and Breast Cancer Phenotypes in Vitro and in Vivo. Cancer Res. 2016, 76, 652–663.

30. Yujiro Tsujita; Akio Horiguchi; Tasaki, S.; Isono, M.; Asano, T.; Ito, K.; Asano, T.; Yoshine Mayumi; Toshihiro Kushibiki. STAT3 Inhibition by WP1066 Suppresses the Growth and Invasiveness of Bladder Cancer Cells. Oncol. Rep. 2017, 38, 2197–2204.

31. Baek, N.; Seo, O. W.; Kim, M.; Hulme, J.; An, S. S. A. Monitoring the Effects of Doxorubicin on 3D-Spheroid Tumor Cells in Real-Time. Onco. Targets. Ther. 2016, 9, 7207–7218.
32. Mittler, F.; Obeïd, P.; Rulina, A. V.; Haguet, V.; Gidrol, X.; Balakirev, M. Y. High-Content Monitoring of Drug Effects in a 3D Spheroid Model. Front. Oncol. 2017, 7, 293.
33. Jung, K. B.; Kwon, O.; Lee, M.-O.; Lee, H.; Son, Y. S.; Habib, O.; Oh, J.-H.; Cho, H.-S.; Jung, C.-R.; Kim, J.; Son, M.-Y. Blockade of STAT3 Causes Severe in Vitro and in Vivo Maturation Defects in Intestinal Organoids Derived from Human Embryonic Stem Cells. J. Clin. Med. 2019, 8, 976.
34. Fiorillo, M.; Ózsvári, B.; Sotgia, F.; Lisanti, M. P. High ATP Production Fuels Cancer Drug Resistance and Metastasis: Implications for Mitochondrial ATP Depletion Therapy. Front. Oncol. 2021, 11.
35. Tošić, I.; Frank, D. A. STAT3 as a Mediator of Oncogenic Cellular Metabolism: Pathogenic and Therapeutic Implications. Neoplasia. 2021, 23, 1167–1178.
36. Bhatti, J. S.; Bhatti, G. K.; Reddy, P. H. Mitochondrial Dysfunction and Oxidative Stress in Metabolic Disorders — a Step towards Mitochondria Based Therapeutic Strategies. Biochim. Biophys. Acta Mol. Basis Dis. 2017, 1863, 1066–1077.
37. Zhang, J.; Yeong Shik Kim; Kim, C.; Shanmugam, M. K.; Kodappully Sivaraman Siveen; Newsholme, P.; Ramar Perumal Samym; Amudha Deivasigamanim; Lina; Wang, L.; Boon Cher Goh; Alan Prem Kumar; Hui, K. M.; Sethi, G. Nimbolide-Induced Oxidative Stress Abrogates STAT3 Signaling Cascade and Inhibits Tumor Growth in Transgenic Adenocarcinoma of Mouse Prostate Model. Antioxid. Redox Signaling. 2016, 24, 575–589.
38. Levy, D. E.; Lee, C. What Does Stat3 Do? J. Clin. Invest. 2002, 109 (9), 1143–1148.
39. Gu, Y.; Mohammad, I.; Liu, Z. Overview of the STAT-3 Signaling Pathway in Cancer and the Development of Specific Inhibitors (Review). Oncol. Lett. 2020, 19, 2585-2594.
40. Fischer, U.; Jänicke, R. U.; Schulze-Osthoff, K. Many Cuts to Ruin: A Comprehensive Update of Caspase Substrates. Cell Death Differ. 2003, 10, 76–100.
41. Kaufmann, S. H.; Desnoyers, S.; Ottaviano, Y.; Davidson, N. E.; Poirier, G. G. Specific Proteolytic Cleavage of Poly(ADP-Ribose) Polymerase: An Early Marker of Chemotherapy-Induced Apoptosis. Cancer Res. 1993, 53, 3976–3985.
42. Li, Y.; Lin, K.; Yang, Z.; Han, N.; Quan, X.; Guo, X.; Li, C. Bladder Cancer Stem Cells: Clonal Origin and Therapeutic Perspectives. Oncotarget. 2017, 8, 66668–66679.